SIGNAL QUALITY MONITORING TO COUNTER RAIN FADING WITH ADAPTIVE INFORMATION BIT ENERGY IN SATELLITE THIN ROUTE TDMA SYSTEMS

Internal Report C95-44

December 1995

Nedo Celandroni
Francesco Potortì
Santi T. Rizzo

Signal Quality Monitoring to Counter Rain Fading with Adaptive Information Bit Energy in Satellite Thin Route TDMA Systems

Nedo Celandroni *
Francesco Potortì *
Santi T. Rizzo #

* CNUCE, Institute of National Research Council
Via S. Maria 36 - 56126 Pisa - Italy
Phone: +39-50-593207/593203
Fax: +39-50-589354 - Telex: 500371
E-mail: n.celandroni@ cnuce.cnr.it
pot@cnuce.cnr.it

CNR fellowship holder at CNUCE

CNUCE REPORT C95-44

December 1995

Keywords: satellite, fade countermeasure, signal quality estimation, attenuation estimation, attenuation model, Kalman filtering, demand-assignment, TDMA access schemes.

Summary. This paper describes a complete fade countermeasure system, based on up-link transmission power control, plus data coding and bit rates variation. The system is designed for thin route TDMA user-oriented satellite networks, used for LAN interconnection. A multicarrier access to the satellite transponder is envisaged to exploit the entire transponder bandwidth with limited data rates of each carrier. The modest performance required by the earth stations means that the antennas can easily be installed on the user's premises. In order to avoid excessive intermodulation noise, the satellite transponder input back-off must be constant and sufficient to operate in the linear zone. This imposes a calibrated action of the up-link power control, which is possible only by knowing the up-link attenuation with good accuracy. The total signal degradation, due to the residual up-link attenuation after up-power control intervention, and to the down-link attenuation, is compensated for by varying the coding and bit rates of the data. A signal to noise estimator, based on the statistics of quantised levels of the demodulated PSK signal and a narrow band signal level estimator are employed to apply the countermeasures that are able to maintain the data bit error rate required by the user. The performance of the whole system is evaluated in an AWGN (Additive White Gaussian Noise) environment, for two similar channel access schemes, which differ in the control type (centralised or distributed) of the channel capacity assignment mechanism.

1. INTRODUCTION

Using the Ka band for satellite communications entails solving the rain fading problem to ensure an acceptable availability of the link. The fade countermeasure system we propose is not very complex and is cost effective compared to some others, such as space [10] or frequency diversity [12-14]. Our scheme is based on the adaptation of the energy per information bit to the channel fading conditions, in order to maintain the quality of data within the requirements specified by the user. The total attenuation of each link (up-link plus down-link) is compensated for by varying the transmission power, coding and bit rates. Assuming a multi-channel TDMA access to the satellite, the transmission power variation must ensure a constant back-off at the transponder input to avoid excessive intermodulation noise. The power control can thus be used to compensate for up-link attenuations only, while the total compensation is completed by varying the coding and bit rates as well.

A very important problem in fade countermeasure systems is the need to detect the signal quality quickly and accurately. In fact, the countermeasure has to be made before the signal degradation affects the bit error rate (BER) realisable by the user. BER monitoring is not a suitable solution because it is not fast enough. The levels of the BER commonly required are in the order of $10^{-6} \div 10^{-8}$, and in any case, for almost all the existing applications whose bit rate is of a few Mbit/s at maximum, quite a long time is needed to detect the BER with sufficient accuracy.

This paper presents a performance evaluation of both the signal quality and the attenuation estimators used in the fade countermeasure system adopted by two similar channel access schemes. The signal quality estimator is based on the statistical level of PSK demodulated signals, while a narrowband signal level estimator is employed to evaluate the attenuation. We assume that we are operating in the presence of additive white Gaussian noise (AWGN) alone: this means that the satellite channel corruption is only due to thermal noise. To improve the performance of both the estimation systems, a Kalman filtering is used as well.

The channel access schemes, which employ the above mentioned estimators, are user-oriented demand-assignment systems operating in TDMA, used for LAN interconnection. They support

both real-time (telephony and video) and non real-time (computer data exchange) application traffic.

One of the two systems, named FODA/IBEA (Fifo Ordered Demand Assignment/Information Bit Energy Adaptive)[1, 2], was developed and tested on the Italsat satellite. It is based on a centralised control of the channel capacity assignment algorithm, according to user demand. The other system, named FEEDERS (Faded Environments Effective Distributed Engineering Redundant Signalling) [4], is an evolution of FODA/IBEA, based on an almost entirely distributed algorithm for the channel capacity assignment. A comparative study of the performance of the two systems is reported in [5] from the point of view of the delay experienced by the non real-time traffic. Here a comparison is made from the point of view of the fade countermeasure system performance.

Both schemes are provided with a master station responsible for system synchronisation and, in the centralised case, for the capacity allocation on request of the traffic stations. To accomplish its task the master sends a reference burst, which contains the transmission times of the single stations (allocations), computed according to specific algorithms for real-time and non real-time capacities, respectively. The reference burst is sent at the beginning of each 20 ms frame in the centralised case, and every fourth frame in the distributed one. In the first case the allocations are computed by the master alone, and the traffic stations receive the allocations two round trips after sending their requests. In the second case, the traffic stations monitor all the requests and compute the allocations simultaneously, so they can transmit only one round trip after sending their requests. In the distributed scheme, each request is repeated four times, in order to reduce dramatically any problems due to misunderstanding the requests. Such impairment are in any case recoverable, but they cause collisions and loss of data. In both systems each active station transmits one burst per frame, containing control information plus any number of data packets with individual parameters, such as address, length, application type, data coding and bit rates. The power of the received reference burst is assumed as the reference level, and all the stations do their best to track it with their own bursts by varying the transmission power. Any up-link

residual attenuation, after Up Power Control, contributes to the total degradation of the signal, in addition to the down-link E_b / N_0 degradation of the receiving station. To compensate for link degradation, data is made redundant by reducing the coding rate first, and then reducing the bit rate as well, if necessary. This countermeasure was developed in the FODA/IBEA system by exploiting a powerful feature of the modem prototype, which can dynamically change the data bit rates on a sub-burst basis. The sub-burst is the sequence of data addressed to a certain station within a data burst. In other words, data is "more expensive" in terms of transmission time duration depending on the weather conditions at the sending and receiving stations, because the redundancy introduced lengthens the burst duration.

The two access schemes have different parameters which affects the performance of the countermeasure system in opposite ways. As we will see, in the centralised scheme the delay between the request and the allocation of the bandwidth is higher than in the distributed scheme. This causes a prediction of the signal degradation for a longer time in the centralised case. On the other hand, the average bit rate of the data used to estimate the signal degradation (reference burst) is lower in the distributed system. These two opposite effect give similar results for the performance of the two access schemes.

This paper is organised as follows. In Section 2 the signal quality estimator and its performance are presented, and in Section 3 a model for the rain attenuation is derived. The results are used in Section 4 to estimate the variance of the prediction of both the signal quality and the up-link attenuation. The optimisation of the measure time interval is made in Section 6, also using a Kalman filter outlined in Section 5. The performance of the overall system for the two similar access schemes is described in Section 7. Conclusions are drawn in Section 8.

All the calculations needed in the present paper were obtained with the mathematical computation package *Mathematica*™ [26].

2. SIGNAL QUALITY ESTIMATOR

The signal quality estimator considered is based on the soft levels of the demodulated signal. Hereafter, we assume that binary PSK is being used, although the analysis can be extended to other PSK modulation schemes, in that they can be considered as being several BPSK sequences.

Figure 1 illustrates the functional block diagram of a digital communication system. The input data is first encoded, then presented to the modulator and converted into a sequence of waveforms. In the channel model considered the transmitted signal *s(t)* is corrupted by an AWGN process *n(t)* (Fig. 2).

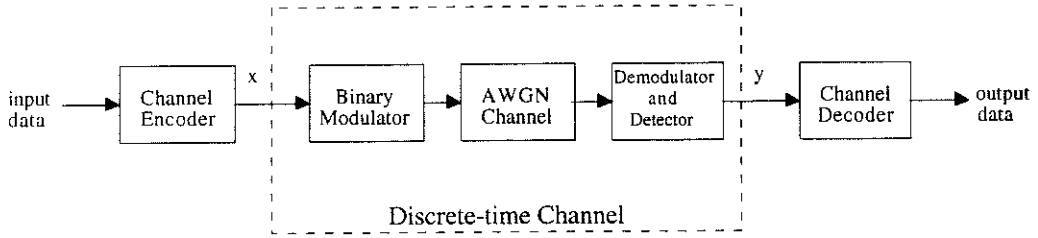

Fig. 1. General channel model for digital communication systems

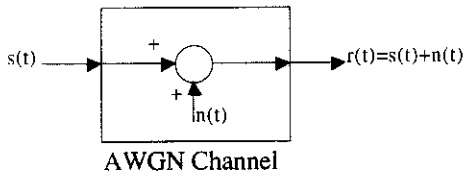

Fig. 2. Channel corruption

At the receiver, the demodulator/detector extracts the binary sequence from the waveforms received. In this context, it is interesting to consider the following cases.

1) The detector, which follows the demodulator, decides on whether the bit transmitted is a 0 or a 1. In this case, the detector makes a *hard decision.* If we see the decision process as a form of quantization, we observe that a hard decision corresponds to a binary quantization of the demodulator output. In this model, the combination modulator-channel-demodulator/detector is equivalent (Fig. 3) to a *binary symmetric channel* (BSC).

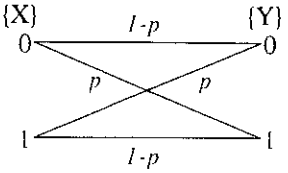

Fig. 3. Binary symmetric channel; p is the probability of error

2) The detector quantizes to $Q>2$ levels (Q-ary detector). In this case, we say that the detector operates a *soft decision*; the combination modulator-channel-demodulator/detector is now equivalent to a binary-input Q-ary output discrete channel (Fig. 4).

3) The demodulator output is unquantized ($Q=\infty$). In this case, the combination modulator-channel-demodulator/detector is equivalent to a binary-input continuous-output channel.

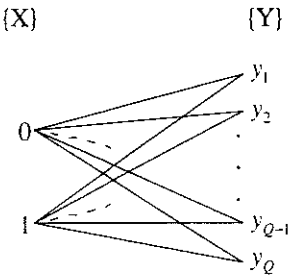

Fig. 4. Binary input Q-ary output channel

For our purposes, we consider the particular case depicted in Fig. 5.

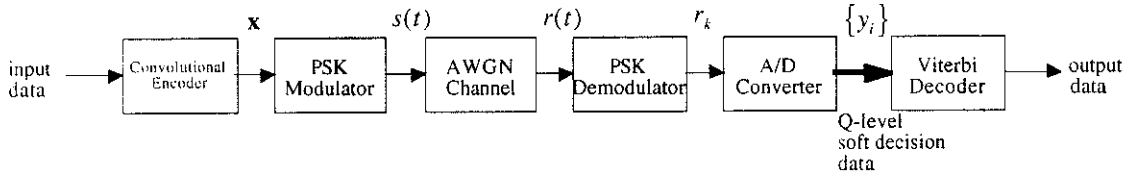

Fig. 5. The channel model considered for the signal quality estimator

In this system, binary PSK modulation and convolutional encoder with Viterbi decoder is employed. To get the highest coding gain, it is preferable to operate in soft decision mode.

The output of the PSK demodulator (matched filter receiver) sampled at the instant t_k may be expressed as:

$$r_k = \begin{cases} \sqrt{E_b} + n_k & \text{when the transmitted bit is a 1 (x = 1)} \\ -\sqrt{E_b} + n_k & \text{when the transmitted bit is a 0 (x = 0)} \end{cases}$$

The random variable n_k represents AWGN at the sampling instant t_k with zero mean and variance $N_0 / 2$ (N_0 is the one sided noise power density), E_b is the energy per bit of the signal transmitted. Consequently, the conditional probability density functions for the two possible signals transmitted ($s_1 = -s_0 = \sqrt{E_b}$) are:

$$p(r_k|s_1) = \frac{1}{\sqrt{\pi N_0}} \exp\left\{ \frac{\left(r_k - \sqrt{E_b}\right)^2}{N_0} \right\}, \qquad p(r_k|s_0) = \frac{1}{\sqrt{\pi N_0}} \exp\left\{ \frac{\left(r_k + \sqrt{E_b}\right)^2}{N_0} \right\}.$$

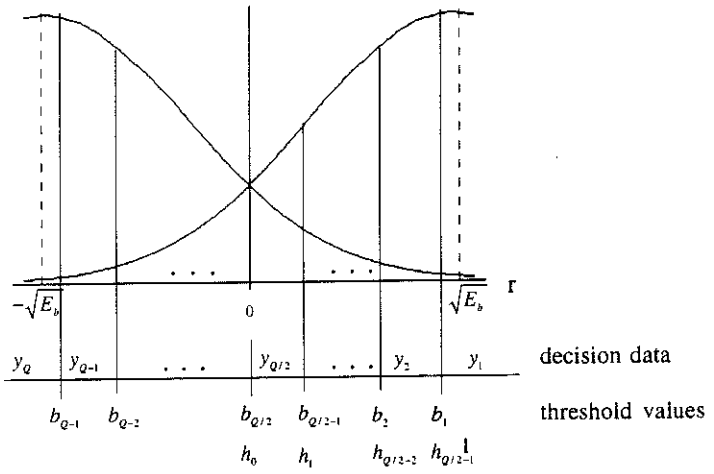

Fig. 6. Probability density function of the signal soft decision levels

The demodulated analog signal is converted into the digital data y_i (i=1,2,..,Q) at the A/D converter based on the pre-determined soft decision thresholds b_1, b_2, ... , b_{Q-1}, as shown in Fig. 6. The Q-level soft decision data y_i obtained is sent to the Viterbi decoder.

By using the conditional probabilities that the signal received falls into a generic quantization interval, for the possible signals transmitted, we obtain the probability for each quantization level (see *Appendix A*):

$$P_i(R)=\frac{1}{2}\left\{erfc\left[10^{R/20}(1-h_i)\right]-erfc\left[10^{R/20}(1-h_{i-1})\right]+erfc\left[10^{R/20}(1+h_{i-1})\right]-erfc\left[10^{R/20}(1+h_i)\right]\right\} \tag{1}$$

$i=1, \ldots, Q/2$

where:

$$h_i=\frac{b_{Q/2-i}}{\sqrt{E_b}}=\begin{cases}\dfrac{i}{Q/2} & i=0, \ldots, Q/2-1\\ +\infty & i=Q/2\end{cases}$$

and R is the E_b/N_0 ratio expressed in dB.

Denoting by q the random variable that associates a weight q_i to each quantization level, we can evaluate the mean and the variance as:

$$\mu_q(R)=\sum_{1}^{Q/2} q_i P_i(R)\ , \tag{2}$$

$$\sigma_q^2(R)=\sum_{1}^{Q/2} q_i^2 P_i(R)-\mu_q^2(R). \tag{3}$$

Let us denote as $\bar{q}$ the sample mean of q over a large number of received bits N. For the central limit theorem $\bar{q}$ has a normal distribution with mean $\mu_{\bar{q}}(R)=\mu_q(R)$ and variance $\sigma_{\bar{q}}^2(R)=\sigma_q^2(R)/N$. The monotonic function $\mu_q(R)$ can be inverted, so we can find $\hat{R}$, such that $\mu_{\bar{q}}\left(\hat{R}\right)=\bar{q}$, where the random variable $\hat{R}$ denotes the estimation of R given $\bar{q}$. Under the hypothesis that $\sigma_{\bar{q}}^2(R)$ is sufficiently small, i.e. such as to allow a local linear approximation, the distribution of $\hat{R}$ can be considered as being normal, with a mean given by $\hat{R}=\mu_{\bar{q}}^{-1}(\bar{q})$, and variance given by:

$$\sigma_{\hat{R}}^2(R)=\frac{\sigma_q^2(R)}{\left(d\mu_q(R)/dR\right)^2 N} \tag{4}$$

For nor negligible values of $\sigma_{\bar{q}}^2(R)$, (4) may be not acceptable and the distribution of $\hat{R}$ cannot be assumed to be normal. A reasonable approximation is to consider the distribution of $\hat{R}$ as still normal, with a mean given by (2), and a raised variance given by:

$$\sigma_{\hat{R}}^2(R) = \frac{\sigma_q^2(R)}{N\left(\Delta\mu_q(R)/\Delta R\right)^2}$$

where $\Delta\mu_q/\Delta R = \min\left\{\left[\Delta\mu_q/\Delta R\right]^+, \left[\Delta\mu_q/\Delta R\right]^-\right\}$; $[\cdot]^+$ and $[\cdot]^+$ are the right and left incremental ratios, respectively, and $\Delta\mu_q = \pm 3\sigma_{\bar{q}}$.

For our purposes, we had to choose the $Q/2$ weights q_i that minimise a certain objective function. In order to simplify the calculation, we can consider a degree α (with $\alpha<Q$ /2-1) polynomial envelope of weights:

$$q(Q/2-i) = c_\alpha i^\alpha + c_{\alpha-1} i^{\alpha-1} + \ldots + c_2 i^2 + c_1 i + c_0 \qquad i = 0,\ldots,Q/2-1 \qquad (5)$$

and determine α +1 coefficients of the polynomial, instead of Q /2 weights.

It is easy to prove that $\sigma_{\hat{R}}^2(R)$ does not change if all the weights are increased by the same quantity or are multiplied by the same factor. Therefore, it is possible to put in (5): $c_1 = 1$, $c_0 = 0$. Thus the minimisation problem is in α-2 variables.

We chose the objective function to minimise as the sum of the variances of $\hat{R}$ taken at the borders and in the middle of the application field. Furthermore, we chose α=2, because a higher degree does not give any significant improvement.

Unfortunately, in our implementation, the reference levels "1" and "0" are affected by a noticeable residual jitter. This impairment does not appreciably degrade the BER performance of the modem and the Viterbi decoder, but does affect the characteristics of our signal quality estimator. In order to optimise the weights, we measured the probabilities of each quantization level by using the modem in IF loop-back with AWGN. We then used these probabilities

instead of the theoretical ones given by (1), and applied the procedure described above to obtain the vector of the weights. Figure 7 shows the characteristics of the signal quality estimator considered, for both theoretical and real cases. The optimised weight vectors are also indicated.

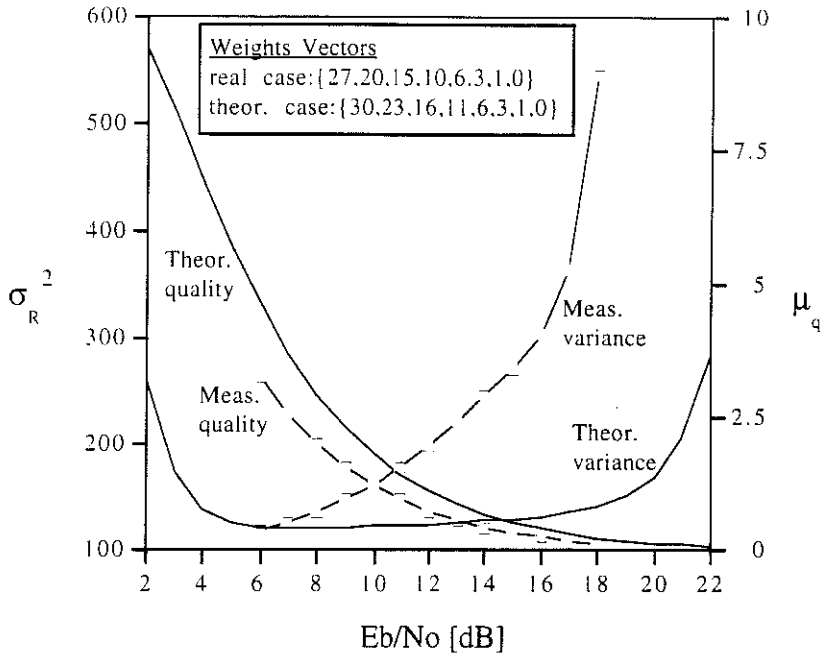

Fig. 7. Mean and variance of the signal quality estimator. Theoretical and real cases.

Note that the signal quality estimator described above was developed with very little additional hardware. In fact, we used the soft levels like those used for the Viterbi decoder. The mean value of the quality random variable is obtained by providing the software with the sum of the levels, each multiplied by the relevant weight, at the end of each data sub-burst. This sum is produced using a network simply made by an EPROM. The software then divides the sum by the total number of bits to get the mean value.

A method which significantly improves the accuracy of the estimator is described in [16]. It is based on extended quantization of the demodulated signal, regardless of the levels used by the Viterbi decoder. It means that the signal levels used by the estimator are extended beyond the

mean values of both the 1 and the 0 levels. This allows us to approximately halve the variance of the estimation, as it is the same as using twice the number of bits. The method proposed in [16], however, does not optimise the weight vector. We think that the solution which produces the best performance is given by using the extended quantization with a weight vector optimised over the application field.

As we will see later, with the parameters used in our case the variance of the signal quality estimator is small enough not to justify a further costly improvement. This can be seen by comparing the overall system performance obtained with and without Kalman filtering, with the measured values of the variance shown in Fig. 7. The modest difference between the two cases proves that a reduction in the measure variance would not produce any significant improvement in the performance.

3. THE ATTENUATION MODEL

Estimating and predicting the signal degradation entails using a model that describes the attenuation process.

We started from a data set chosen from the results of the propagation experiment, in Ka band, carried out on the Olympus satellite by the CSTS (Centro Studi sulle Telecomunicazioni Spaziali) Institute, on behalf of the Italian Space Agency (ASI). The up-link (30 GHz) and down-link (20 GHz) attenuation values considered were taken at 1 s intervals and averaged over the same interval. The samples are relevant to 10 significative events for a total of 170,000 s recorded at the Spino d'Adda (North of Italy) station.

The attenuation behaviour observed recalls the behaviour of a self-similar process (see below for a pictorial assessment), so an attempt is made here to model the attenuation process as a fractal Brownian motion [25]. The process parameters were computed using the following procedure.

Let us firstly denote by A a generic attenuation and by R the E_b / N_0 ratio. The sub-scripts u and d refer to up-link and down-link parameters, respectively. The above quantities are expressed in dB when a capital letter is used. For example, for the down-link attenuation we have: $A_d = 10\ Log_{10} a_d$.

We divide the entire sample data into attenuation belts, with an amplitude of 1 dB for the down- and 2 dB for the up-link attenuation, respectively.

We consider the process $W(t_1,\ t_2)$, which gives the difference of the attenuation between the instants t_2 and t_1. Our basic assumption is that while process W belongs to the same belt, it only depends on the time difference $t = t_2 - t_1$. Thus, denoting by A_n the attenuation at the centre of the n^{th} belt, we have: $W(t_1,\ t_2,\ A_n) = W(t,\ A_n)$.

The available data gives samples of the attenuation process at instant multiples of 1 s, i.e. we only have $W(m\Delta t, A_n)$, with Δt= 1 s and m integer.

For each pair of values m and A_n, the process W is assumed as: $N(0, \sigma_W^2)$, where σ_W^2 denotes the variance of the process W. In fact the Chi-Square test [17], for values of m = 1, 2 and 3, gives acceptable results, i.e. in the order of 1-5% level of significance. Unfortunately, while the lower belts are very rich in samples, the higher ones are not and in these cases the above assumption cannot be completely justified. Due to the insufficient volume of data, we limit our analysis to the attenuation values that give an acceptable number of samples. Fixing this number to 300, the attenuation limits are 30 dB for up-link and 16 dB for down-link, respectively.

Fractal Interpolation.

We need some method of interpolating the results because, for our purposes, the 1 s spacing is too wide. By visual inspection and by analogy with many natural phenomena [25], we approximate the attenuation process with a fractional Brownian motion. We begin by computing the Hurst parameter of the attenuation process, then we show a visual justification of our hypothesis.

We assume that the variance of the W process can be expressed as:

$$\sigma_W^2 = C + V\ t^{2H}, \qquad (6)$$

where the coefficients H (said Hurst coefficient), V and C generally depend on A_n.

To evaluate such coefficients, $\sigma_W^2(t,\ A_n)$ is computed for a number of A_n values lying between 1 and $A_{n_{max}}$, and for the time values of 1, 2 and 3 s. For each value of the time, the points are then interpolated with a polynomial to a smooth the data. The coefficients H, V and C are thus obtained by using a non-linear least square method. The coefficient C should not appear in the fractal Brownian model. It represents the variance of the process W at $t = 0$, so it should be theoretically null. A non null value of C is justified as the sum of the residual contribution of the scintillation effect, plus the measurement error. The attenuation samples, in fact, are averaged over 1 s intervals, so only a part of the scintillation spectrum [27] is included. The scintillation and the error processes are assumed to depend on frequency alone. Thus, for each

frequency, C is the sum of the two variances. The observed variability of C with A_n is only due to measurements, so we take their mean value $\overline{C}$. The new expression for σ_W^2 is then

$$\sigma_W^2 = C_1 + V(A_n)\ t^{2H(A_n)} \qquad (7)$$

The coefficients H and V are then recomputed by using a non-linear least square error method and the coefficient $\overline{C}$ must be excised from the rain attenuation model. Therefore, in order to have a complete model, $\overline{C}$ is replaced by a different value C_s, which takes into account the all the contribution due to scintillation. This contribution is assumed to have a variance constant with the attenuation and, and is dependent on frequency alone.

Let us interpolate with polynomials the points which give the value of the coefficients as functions of A_n, and let the subscript u denote the up-link and subscript d the down-link cases, respectively. Finally, we have:

$$\sigma_W^2 = C_s + V(A)\ t^{2H(A)} \qquad (8)$$

where V is interpolated as: $\begin{cases} V_u = 1.9\ 10^{-2} - 1.9\ 10^{-5} A_u + 2.3\ 10^{-5} A_u^2 + 7.2\ 10^{-6} A_u^3 \\ V_d = 0.015 - 0.0022 A_d + 0.00035 A_d^2 \end{cases}$

H is linearly interpolated as: $\begin{cases} H_u = 0.38 + 0.0093 A_u \\ H_d = 0.32 + 0.015 A_d \end{cases}$

Figure 8 reports the points and the interpolating polynomials of the V and H coefficients as functions of the attenuation. The scintillation contribution C_s is chosen as: $C_{s_u} = 0.03$ and $C_{s_d} = 0.02$.

Once the H parameter has been computed, let us draw the attenuation measured at different time scales. Figure 9 shows four different portions of the attenuation time sequence, each one scaled with the correct H parameter. It can be seen how they exhibit similar looking properties, i.e., they look similar to the eye. This property is characteristic of self-similar processes; that is why we chose a fractional Brownian motion model.

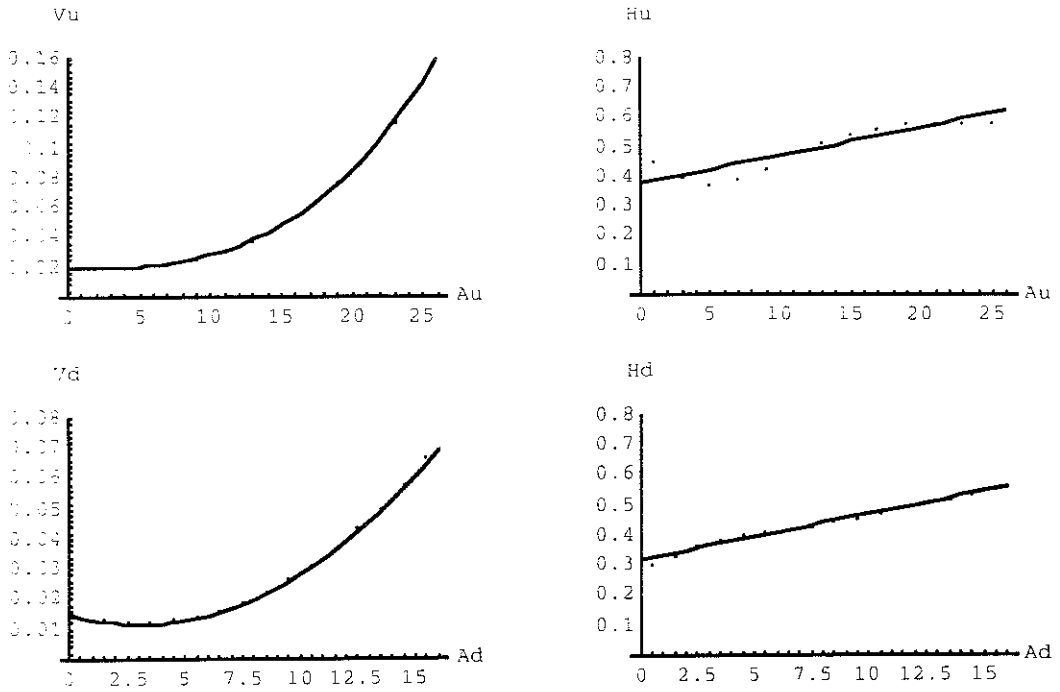

Fig. 8. Interpolation of the coefficients V and H as functions of up and down-link attenuations.

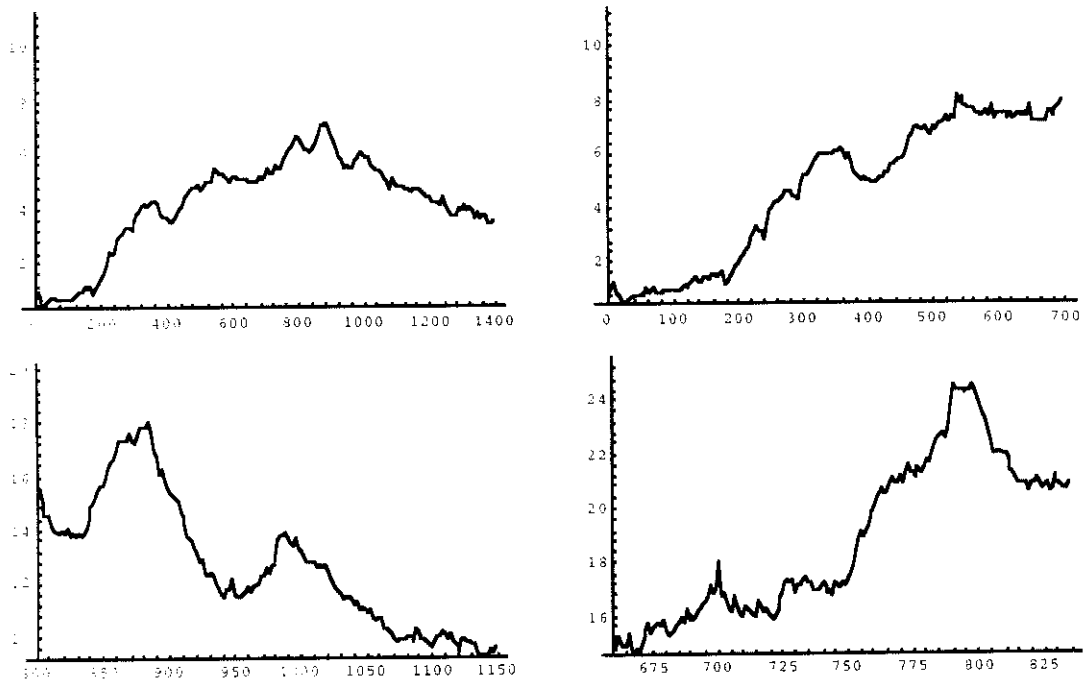

Fig. 9. Rescaled portions of the attenuation time sequence.

4. SIGNAL DEGRADATION PREDICTION

The compensation for both up and down-link attenuations must be done by considering the total degradation of the signal, i.e. the resulting E_b / N_0 available at the receiving station input. Since all the stations must keep a constant power level at the satellite transponder input, the up- and down-link attenuation contributions can be estimated separately. Each receiving station must predict its E_b / N_0 ratio for the receiving time, conditioned to the nominal power available at the transponder input, which is the reference power level sent by the master station. Each transmitting station must thus add, to the down-link degradation level of the receiving station, the contribution due to any up-link degradation predicted for the transmitting time. The total degradation level is used to compute the code and bit rates of the transmitting signal, needed to ensure the BER performance required by the user [1]. The up-link degradation is actually any attenuation portion which remains uncompensated, due to the insufficient power reserve of the transmitting station. A suitable margin due to the prediction errors must be considered, in addition to the degradation level computed as well. The evaluation of this margin and the strategies to minimise it are the subject of the rest of the paper.

First we deal with the E_b / N_0 predicted by the receiving station. Let us consider the process $\Delta_{R_r}(A_d, t)$ defined, similarly to W, as the difference, at the receiving station input, between two values of E_b / N_0 at two time instants, whose difference is t, when the reference power level R_r is received at the satellite transponder, and the down-link attenuation is A_d.

To evaluate the variance $\sigma^2_{R_r}(R_r, t)$ of the process Δ_{R_r}, we consider the relation which gives the resulting E_b / N_0, denoted by r:

$$r = \frac{r_u r_d}{r_u + r_d + 1}. \qquad (9)$$

For simplicity we consider: $r_d = r_{d_c} / a_d$, where r_{d_c} is the reference value in clear sky conditions. This relation is approximated in that the variation of the equivalent noise temperature with a_d is neglected. The condition of a constant reference power level received at the satellite

input implies that r_u is equal to the reference value r_{u_c}, so the reference E_b / N_0 at the station input is:

$$r_r = \frac{r_{u_c} r_{d_c}}{a_d (r_{u_c} + 1) + r_{d_c}}. \qquad (10)$$

We limit our analysis to the linear case, i.e. we suppose that the amplitude of the down-link attenuation difference process W_d is small enough to justify the relation:

$$\Delta_{R_r} = W_d \frac{dR_r}{dA_d}. \qquad (11)$$

Assuming that dR_r / dA_d is constant within each sufficiently small interval of A_d, the distribution of Δ_{R_r} within the correspondent R_r interval, given by (10), can be assumed to be Gaussian, like the distribution of W_d. Thus, considering (11), we can assume that the variance of Δ_{R_r} is:

$$\sigma^2_{R_r}(R_r,\ t) = \sigma^2_{W_d}(R_r,\ t)\left[\frac{dR_r}{dA_d}\right]^2 \qquad (12)$$

Let us now see the effect of the up-link attenuation on r. Due to the multicarrier access to the transponder, the satellite HPA (high power amplifier) must operate in the linear zone, without automatic gain control. We can thus consider the satellite transponder as a linear device, and hence we have:

$$r_u = \frac{r_{u_c}}{a_{u_r}}, \qquad r_d = \frac{r_{d_c}}{a_{u_r} a_d},$$

where a_{u_r} is the residual up-link attenuation after up-power control, i.e.: $A_{u_r} = \max[0,\ (A_u - A_{p_r})]$, where $[0, A_{p_r}]$ is the up-power control range.

The expression which gives r is then:

$$r = \frac{r_r r_{u_c} (1 + r_{u_c})}{a_{u_r} (r_r - a_{u_r} r_r + a_{u_r} r_{u_c} + r^2_{u_c})}$$

However, if we neglect the unity at the denominator of (9), the expression for R is reduced to :

$$R = R_r - A_{u_r}, \qquad (13)$$

i.e. the dB contribution of the residual up-link attenuation can be simply subtracted by the reference E_b / N_0, to get the resulting E_b / N_0 available at the receiving station input. The above approximation causes a maximum error in the order of, for example, a quarter of dB, when the minimum operating value of R is 6 dB.

As data is sent at a certain time after the last estimation of the signal quality, the signal degradation needs to be predicted, in order to choose the most suitable data transmission parameters. The Kalman method is not applicable for prediction because, as we will see, the system model considered does not have a free evolution. Furthermore, we observed that a linear prediction actually worsens the results with respect to the assumption of stationariness. This is due to the particular behaviour of the attenuation process. In fact, whenever an inversion of the process tendency occurs (which actually happens very often), the error on the prediction is bigger than the one made considering the process as invariant since the last estimation. The margin to take into account must be large enough to absorb this error. More sophisticated prediction methods have not as yet been investigated.

We propose the following simple procedure, in which only the last estimation of the process is considered and its variance is predicted for the time suitable. A Kalman filtering is used to produce the optimum estimation of the process. In summary, first the process optimum estimation $\hat{x}$ is produced, together with its variance $\sigma^2_{\hat{x}}$ at the instant t, then the variance is propagated for the instant $t+\tau$ in which data is sent. Assuming a complete incorrelation between the measurement error and the process evolution, the resulting variance is:

$$\sigma^2_r = \sigma^2_{\hat{x}} + \sigma^2_\tau \qquad (14)$$

where σ^2_τ is given by (8) with $t = \tau$, directly when the process A_u is considered, and from (12), after substituting the variance given by (8) when the process R_r is considered.

The R process is estimated with the soft level quality estimator, whose performance is shown in Fig. 7, while A_u is estimated by measuring the power level of the signal received with a narrow-band carrier envelope detector. This device uses most of the hardware already employed for the demodulation, in particular the fast AGC, which builds the data reference level. The bandwidth of this detector was fixed at 1/64 of the signal bandwidth, as a compromise between the noise excision and the ability to reach the steady state level even when the output sampling instant occurs at the end of the shortest burst in play.

5. THE KALMAN FILTER USED

As shown in Fig. 10 we assume that the process (e.g. attenuation) to be estimated $\{ x_k \}$ can be modelled as a first-order recursive process, driven by a zero-mean white noise process $\{ w_k \}$ [22]. Therefore, the attenuation evolves in time according to the dynamic equation:

$$x_{k+1} = x_k + w_k$$

where the subscript is a time argument.

The random drive is specified by:

$$E[w_k] = 0$$

$$E[w_k w_j] = \begin{cases} 0 & k \neq j \\ \sigma^2_{w_k} & k = j \end{cases} \qquad (15)$$

Further, we assume a linear observation model, i.e. the measure of the process, described by:

$$z_k = x_k + v_k$$

where v_k represents an independent additive white noise with zero-mean and variance $\sigma^2_{v_k}$.

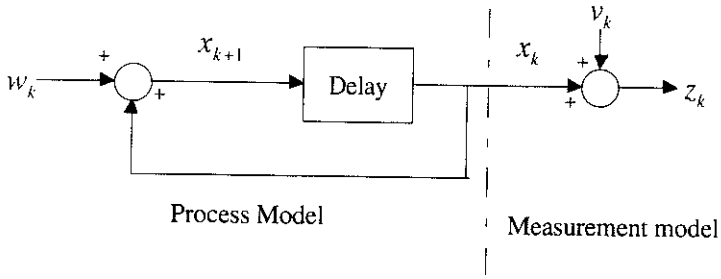

Fig. 10. System model considered.

We also assume that we have an initial estimate of the process at some point in time t_k, and that this estimate is based on all our knowledge about the process prior to t_k [20]. This prior estimate is denoted as $\hat{x}_k^-$. Let us suppose we know the error variance associated with $\hat{x}_k^-$:

$$p_k^- = E\left[\left(x_k - \hat{x}_k^-\right)^2\right]$$

With the assumption of a prior estimate $\hat{x}_k^-$, we can use the measurement z_k to improve the prior estimate by choosing a linear blending of the noisy measurement and the prior estimate in accordance with the equation:

$$\hat{x}_k = \hat{x}_k^- + K_k\left(z_k - \hat{x}_k^-\right)$$

where: $\hat{x}_k$ = updated estimate; K_k = blending factor (to be determined).

The particular K_k that minimises the mean square estimation error (or error variance associated with the updated estimate)

$$p_k = E\left[\left(x_k - \hat{x}_k\right)^2\right]$$

is called the *Kalman gain.*

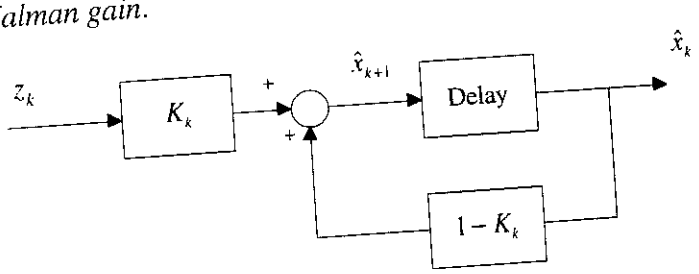

Fig. 11. The Kalman filter model.

Starting with the initial conditions:

$$p_1 = \sigma_{v_1}^2, \qquad K_1 = 1, \qquad \hat{x}_1 = z_1,$$

the Kalman filter recursive loop is the following (Fig. 11):

$$\begin{cases} \hat{x}_{k+1}^- = \hat{x}_k, \quad p_{k+1}^- = p_k + \sigma_{w_k}^2 & (\textit{project ahead}) \\ p_{k+1} = \dfrac{p_{k+1}^- \sigma_{v_{k+1}}^2}{p_{k+1}^- + \sigma_{v_{k+1}}^2} & (\textit{compute error} \text{ variance}) \\ K_{k+1} = \dfrac{p_{k+1}}{\sigma_{v_{k+1}}^2} & (\textit{compute Kalman gain}) \\ \hat{x}_{k+1} = \hat{x}_{k+1}^- + K_{k+1}\left(z_{k+1} + \hat{x}_{k+1}^-\right) & (\textit{update estimate}) \end{cases} \tag{16}$$

Note that assumption (15) is not fully respected, because our process is not pure Brownian, as in this case the Hurst coefficient would be identically equal to 0.5. The general diversity of H from the value 0.5 and more importantly the presence of the coefficient C_s in relation (8) cause a

violation of assumption (15). The application of Kalman filtering without taking this into account, produces only a sub-optimal solution, which does however improve the overall performance.

The Kalman filter behaviour is shown in Fig. 12 for a wide range of ratios between the measured and the process variances. The figure highlights the reduction in error variance induced by the filter. As the convergence of the Kalman filter is quite fast, a steady-state determination is presumably achieved before a significant change in the estimated process occurs. Thus we can assume that after a few initial steps, each determination approximates the steady-state condition.

At steady-state we have:

$$p_{k+1} = p_k = p^*$$

and from the second and third of (16) we obtain the approximated error variance p^* of each determination as:

$$p^* = \frac{\sigma_w^2}{2}\left(\sqrt{1+4\frac{\sigma_v^2}{\sigma_w^2}}-1\right) \qquad (17)$$

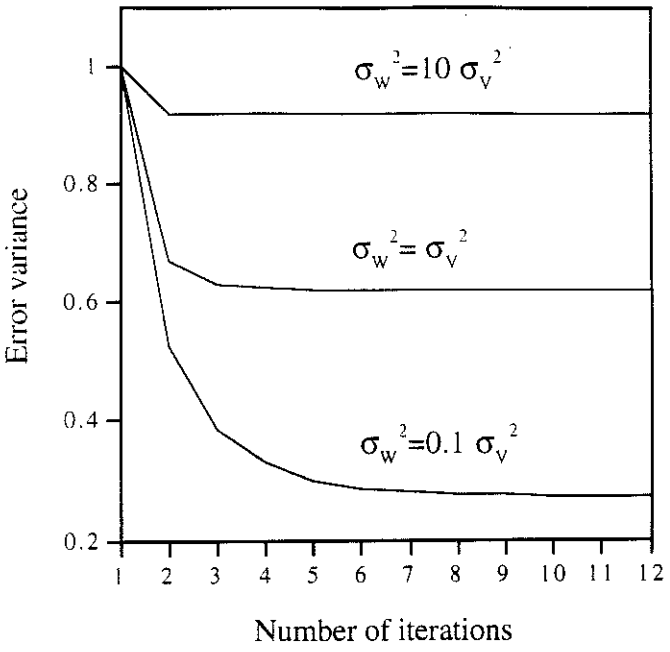

Fig. 12. Error variance in the estimation as a function of the Kalman loop iterations. Different process and Kalman variance ratios are considered.

6. MEASURE TIME OPTIMISATION

Both the variances in the right hand side of (14) depend on the measure time. Let us look at the optimisation of this time, on both down and up sides separately, in order to achieve the minimum variance of the signal degradation prediction.

When Kalman filtering is applied, if assumption (15) were fully respected, it would make no sense to speak about measure time optimisation, since this time should be as small as possible to minimise the variance of the estimation. The assumption of relation (8) as a descriptor of our process, produces either sub-optimal results or optimal measure times different from zero.

Down-link

The predicted variance of R_r can be expressed as:

$$\tilde{\sigma}^2_{R_r} = \sigma^2_m(R_r,\ b_r,\ \tau_m) + \sigma^2_{R_r}(R_r,\ \tau_d + \tau_m), \qquad (18)$$

where: $\sigma^2_m = \dfrac{\sigma^2_{\hat{R}}(R_r)}{b_r \tau_m}$, $\sigma^2_{\hat{R}}$ is the bit quality variance shown in Fig. 7, b_r is the average bit rate of the bit sequence employed for the estimation, τ_m is the measure interval time, $\sigma^2_{R_r}$ is taken from (12), and τ_d is the average delay between the estimation of R_r and the reception of data with transmission parameters based on that estimation. On average, each estimation refers to a time $\tau_m / 2$ in advance and its validity lasts τ_m, so the average delay between measuring and data reception is $\tau_d + \tau_m$. When Kalman filtering is applied, σ^2_m is replaced in (17) with the output of (16), where σ^2_V is replaced by σ^2_m, and σ^2_W is replaced by (12), with $t = \tau_m$.

Up-link

A_u is estimated by the traffic stations by comparing the power level of the reference burst and the level of their own bursts. We assume that the reference burst always has the nominal level, because we assume that the master never experiences severe fading, so that its power reserve is enough to compensate for any up-link attenuation. In fact, there is at least one other standby

station that can take the role of master whenever the current master cannot accomplish its task because of excessive fading. In each traffic station we have:

$$A_u = \Delta p_{cp} + A_{u_r},$$

where Δp_{cp} is the dB difference between the power needed in clear sky conditions and the power actually transmitted as a best effort to track the reference burst level.

The master can measure the sum of its up- and down-link attenuations by comparing the power of the reference burst received with the nominal level for clear sky conditions. In order to estimate its A_u the master uses a beacon receiver to measure A_d. The beacon receiver operates in continuous mode, so its bandwidth has less restrictive limits than the signal level estimator which operates on actual data, and hence in burst mode. The dB variance of each signal level sample, at the output of the low-pass filter, is (see Appendix B)

$$\sigma_s^2 = \left[4.343 \sqrt{\frac{2N_0}{E_b \alpha_b}} \right]^2 \qquad (19)$$

where α_b is the ratio between the signal and the low-pass filter bandwidths. Relation (19) is also applicable to samples of the beacon receiver output.

The variance of A_u prediction made by the master is:

$$\tilde{\sigma}_{MM}^2 = \sigma_{s_M}^2 (R_r,\ \tau_{s_M},\ \tau_{m_M}) + \sigma_{A_u}^2 (A_u,\ \tau_{rt} + \tau_{m_M}), \qquad (20)$$

where: $\sigma_{s_M}^2 = \dfrac{[\sigma_{sl}^2(R_r) + \sigma_{bl}^2(R_r)]\tau_{s_M}}{\tau_{m_M}}$, σ_{sl}^2 is the variance of the signal level estimator, σ_{bl}^2 is the variance of the beacon level estimator, whose bandwidth is assumed to be 1/8 of the signal level estimator bandwidth, τ_{s_M} is the sampling interval time of both the signal and the beacon levels, τ_{m_M} is the measure interval time of the master, and the second term is the contribution of the process evolution, taken by (8). The presence of τ_{rt}, the satellite round trip time, is due to the fact that received data experiences up-link attenuation at a time τ_{rt} in advance. When Kalman

filtering is applied, $\sigma^2_{s_M}$ is replaced in (19) with the output of (16), where σ^2_V is replaced by $\sigma^2_{s_M}$, and σ^2_W is replaced by (8), with $t = \tau_{m_M}$. After each measure, the up-link power is tuned-up accordingly.

The variance of A_u prediction made by each traffic station is:

$$\tilde{\sigma}^2_{A_u} = \tilde{\sigma}^2_{MM} + \sigma^2_{s_T}(R_r, R, \tau_{s_M}, \tau_{s_T}, \tau_{m_T}) + \sigma^2_{A_u}(A_u, \tau_{d_u}), \qquad (21)$$

where: $\sigma^2_{s_T} = \dfrac{\sigma^2_{MT}(R_r)\tau_{s_M} + \sigma^2_{TT}(R)\tau_{s_T}}{\tau_{m_T}}$, σ^2_{MT} and σ^2_{TT} are the variances of the signal level estimated by the traffic station when the master (reference) burst or its own burst is received, respectively, τ_{s_M} and τ_{s_T} are the relevant sampling times, τ_{m_T} is the measure interval time, and τ_{d_u} is the delay between the estimation of A_u and the reception of data. The last term is the contribution due to the process evolution computed by (8). As in the master case, when Kalman filtering is applied, $\sigma^2_{s_T}$ is replaced in (20) with the output of (16), where σ^2_V is replaced by $\sigma^2_{s_T}$, and σ^2_W is replaced by (8), with $t = \tau_{m_T}$.

7. COMPARISON OF THE RESULTS

Table I reports the values of the parameters used for both FODA/IBEA and FEEDERS systems.

PARAMETER	FODA/IBEA	FEEDERS
RB bit rate	2 Mbit/s	
TB initial bit rate	2 Mbit/s	
data bit rate	variable: 8, 4, 2, 1 Mbit/s	
data coding rate	variable: 1/2, 2/3, 4/5, 1	
RB length	1000 bit	800 bit
frame length	20 ms	
RB repetition period: τ_{s_M}	20 ms	80 ms
b_r	50 Kbit/s	10 Kbit/s
τ_{rt}	250 ms	
τ_{s_t}	20 ms	
τ_{d_d}	1,250 ms (5 τ_{rt})	750 ms (3 τ_{rt})
τ_{d_u} (full A_u compensation)	250 ms (τ_{rt})	
τ_{d_u} (partial A_u compensation)	750 ms (3 τ_{rt})	500 ms (2 τ_{rt})
$R_{u_c} = R_{d_c}$	21 dB	
RB E_b / N_0 in clear sky	18 dB	
TB E_b / N_0	max.: 12 dB (clear sky); min.: 6 dB	

TABLE I. *Values of the parameter used. RB:Reference Burst; TB: Transmission Burst.*

The E_b / N_0 ratio chosen equal to 12 dB as a reference value in clear sky conditions gives a BER of 10^{-8} with uncoded data. This BER can be maintained up to 6 dB by using lower coding rates. The gain in reducing the data rate from 8 to 1 Mbit/s is 9 dB, so the gain of the code plus bit rate variations is 15 dB, which added to 10 dB of up power control range gives a 25 dB span for the fade countermeasure considered. Figure 13 shows the temporal schemes which justify the delays assumed for the variance predictions of R_r and A_u. The results of these computation s are reported in Figs. 14-17 for the two systems considered, and for both up- and down-link cases, respectively.

DOWN-LINK

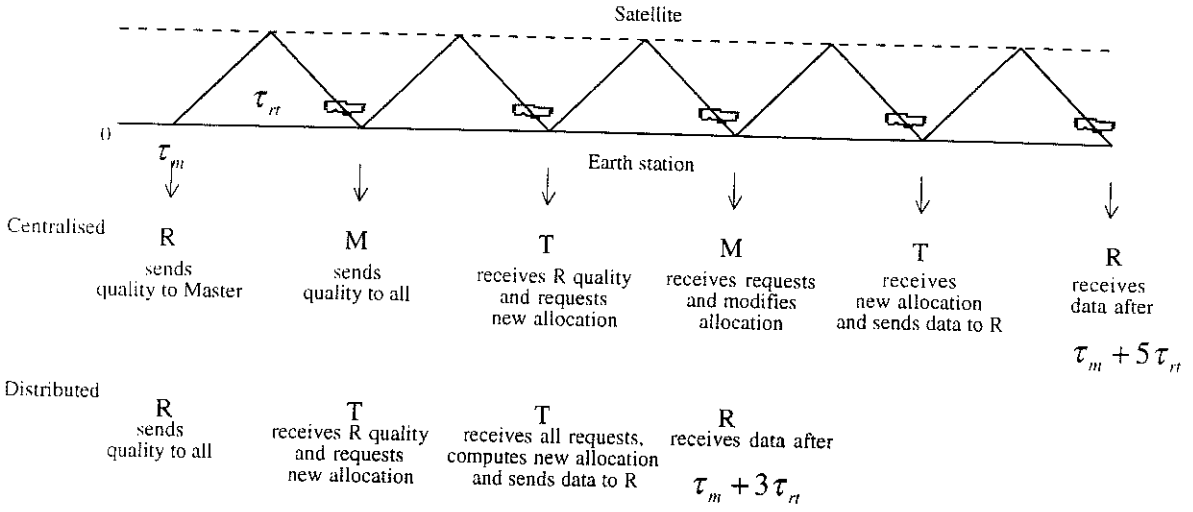

UP-LINK

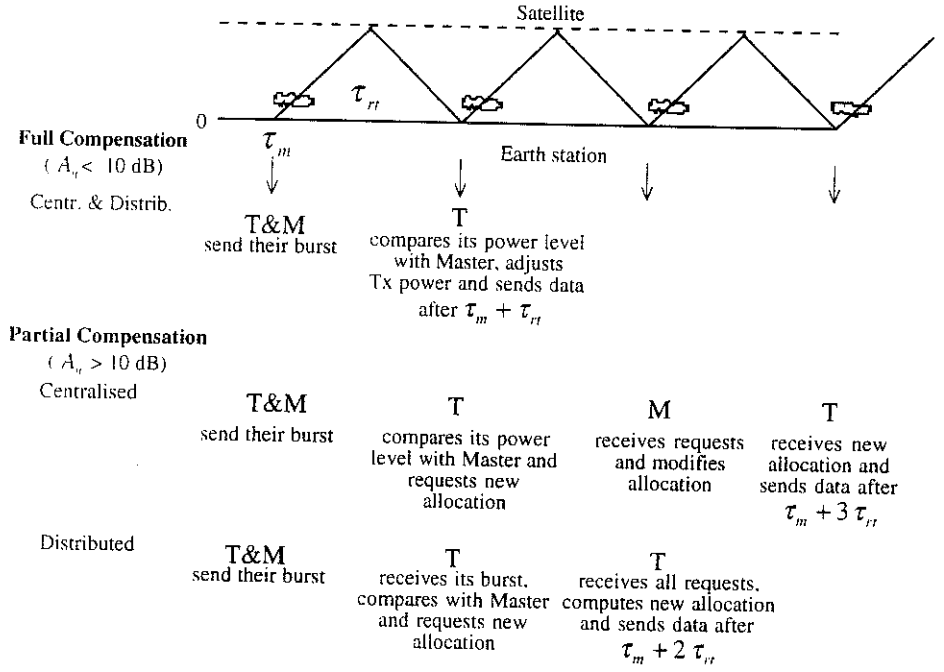

FIG. 13. Temporal scheme for prediction of reference E_b / N_0 (down-link) and up-link attenuation in centralised and distributed cases. M, R and T denote the master, receiving and sending stations, respectively.

These figures show the improvement obtained by applying Kalman filtering to estimate the processes. The optimum measure interval times, obtained with and without filtering, are reported as well. All the quantities shown are plotted as functions of R_r and A_u, for the down-link and up-link degradations, respectively. The procedure to compute the predicted variances is as follows.

The variance of R_r is obtained by minimising (17), using τ_m as a parameter and taking the real case values for the bit quality variance shown in Fig. 7. The values of τ_m, which appear in the relevant figures, are rounded to the closest multiple of the reference burst repetition period.

In the up-link, the variance of the master reference level predicted is obtained by minimising (20) . In order to express the result as a single variable function we assume:

$$A_d = 0.5\ A_u, \qquad (22)$$

using the frequency scaling formula given in [11], which is valid on a long-term basis only. This assumption, however, greatly simplifies the calculations, but does not appreciably affect the results. Looking at Figs. 14 and 15 we can see that the variance of the master does not vary significantly for attenuations below 10 dB, i.e. below the full up-link compensation limit, within which we assume that the master operates. We can thus assume that $\tilde{\sigma}^2_{MM}$ in (21) is constant and equal to the 10 dB value. The variance of A_u, predicted by each traffic station, is then obtained by minimising (21) with assumption (22).

Let us now see how the variances predicted are used in practice. Each traffic station broadcasts its R_r estimate to all the others. The sending station estimates its A_u and computes R using relation (13). Then it decreases R by a margin value M, which depends on the chosen probability p_s that the BER falls below the specified value. Denoting by σ^2_R the variance of the R estimation , we have : $M = K\sigma_R$, where K is such that: $erfc(K) = p_s$.

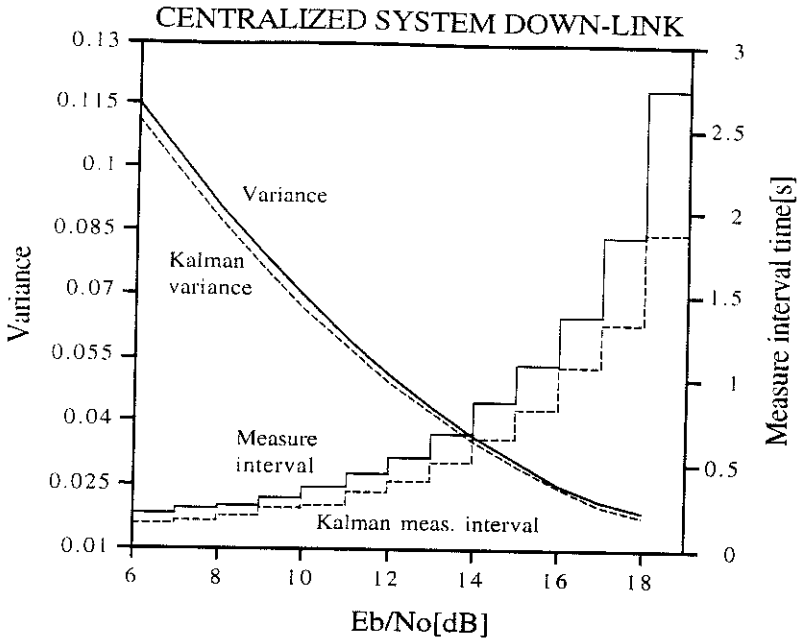

Fig. 14. Variance of the reference E_b / N_0 and relevant optimum measure time. Results of the centralised case, obtained with and without Kalman filtering, respectively.

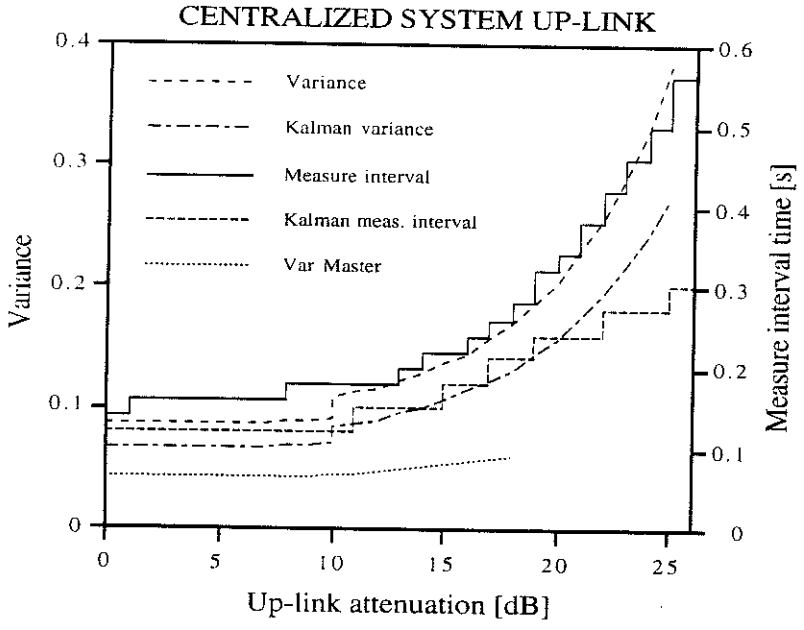

Fig. 15. Variance of the up-link attenuation and relevant optimum measure time. Results of the centralised case, obtained with and without Kalman filtering, respectively. The master up-link attenuation variance is shown as well.

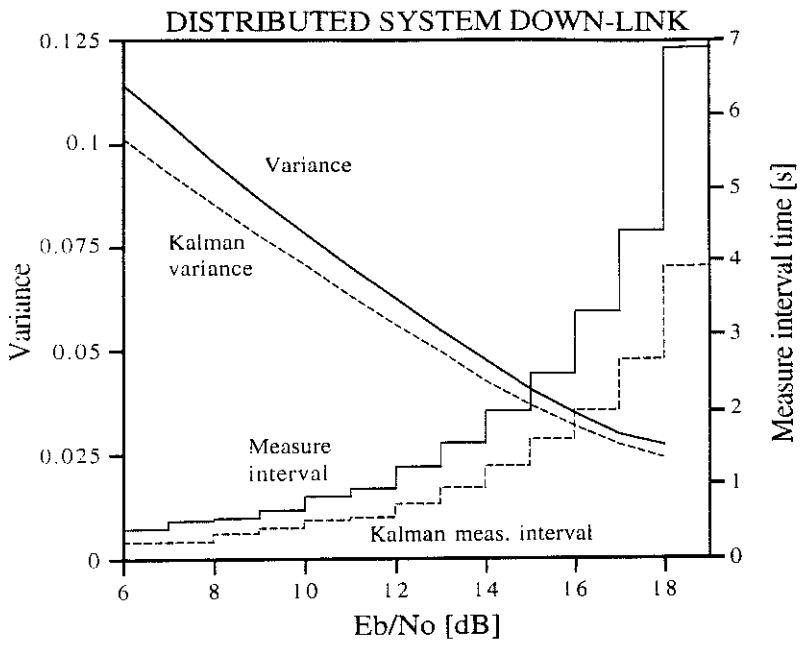

Fig. 16. Variance of the reference E_b / N_0 and relevant optimum measure time. Results of the distributed case, obtained with and without Kalman filtering, respectively.

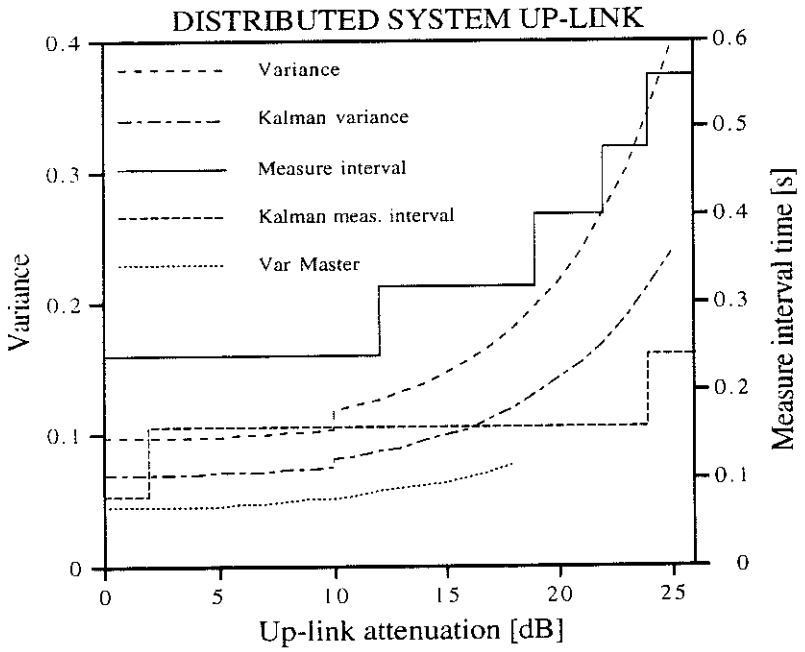

Fig. 17. Variance of the up-link attenuation and relevant optimum measure time. Results of the distributed case, obtained with and without Kalman filtering, respectively. The master up-link attenuation variance is shown as well.

The most reasonable estimation of σ_R^2 is done by assuming a complete incorrelation between processes W_{tt} and Δ_{R_r}. Thus we have:

$$\sigma_R^2 = \tilde{\sigma}_{R_r}^2 + \tilde{\sigma}_{\Delta_{tt}}^2. \qquad (23)$$

Finally, the resulting R is used to choose the appropriate coding and bit rates of the data to send, according to the required BER. From an implementational point of view, as all the above calculations must be done in real-time for each individual transmission, a set of look up tables is employed to get a fast result.

In order to provide a quick means of evaluation, Figs. 18 and 19 show the value of the margin M for two levels of the probability p_s that the BER is greater than the one specified by the user. In Fig. 18 we assume that the receiving station has no attenuation at all (R_r=18 dB) and M is reported here as a function of the sending station up-link attenuation. In Fig. 19 we assume that the sending station experiences an up-link attenuation lower than 10 dB (full compensation) and M is reported as a function of the receiving station reference E_b / N_0. In both figures, the results obtained with and without Kalman filtering application are reported for comparison. Note that the application of the Kalman filtering gives after all a modest reduction of the required margin M. This is principally due to the optimisation of the measure interval times in both the cases and to the small variances of the estimators with respect to the variances of the attenuation process evolution. A more relevant gain of the Kalman filtering would be produced with significantly lower average bit rates of the data used for the estimations.

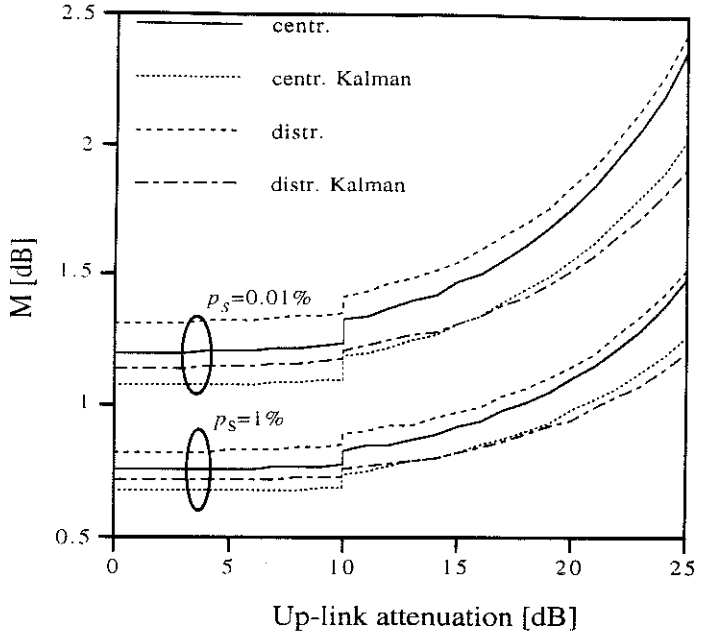

Fig. 18. Margin to take into account over the estimation of the up-link attenuation as a function of the up-link attenuation itself. Both centralised and distributed cases, with and without Kalman filtering, are shown for two different values of p_s.

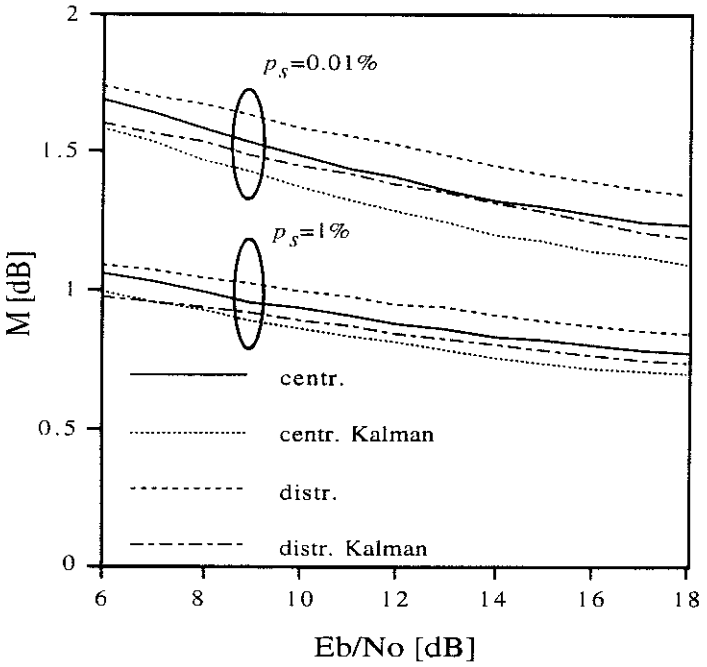

Fig. 19. Margin to take into account over the estimation of the reference E_b / N_0 *as a function of* E_b / N_0 *itself. Both centralised and distributed cases, with and without Kalman filtering, are shown for two different values of* p_s.

8. CONCLUSIONS

We have shown the performance of a complete fade countermeasure system, applied in a centralised and in a distributed control TDMA access scheme. The most relevant characteristic of our system is the use of a margin, which can be varied with the attenuation, in the estimation of the overall signal to noise ratio. This margin varies from values close to 1 dB to values of almost 2.5 dB, depending on different cases. The principal cause of the required margin variation is the attenuation. Thus using a margin which is made variable with the attenuation itself gives a considerable gain. In fact, the system spends most of the time in almost unfaded conditions and the average value of the margin is very close to the minimum value. The margin reduction using the Kalman filter is modest in the cases considered, but this feature is completely implemented by the software and does not increase costs. In the distributed case, the reduced bit rate of the data used to estimate signal degradation is fully compensated for by the reduced propagation time of the attenuation process variances and by the higher gain obtained by using the Kalman filter.

APPENDIX A

The conditional probabilities that the received signal r_k falls into the interval $C_i = [b_{i-1}, b_i]$, for the possible transmitted signals, coincide with the channel transition probability that output symbol y_i is received when input bits $x = 1$ and $x = 0$ are transmitted, respectively. Thus we have:

$$P(r_k \in C_i | s_1) = P(y = y_i | x = 1) = \frac{1}{\sqrt{\pi N_0}} \int_{b_{i-1}}^{b_i} \exp\left\{ \frac{\left(r_k - \sqrt{E_b}\right)^2}{N_0} \right\} dr_k =$$

$$= \frac{1}{2} \left[erfc\left(\frac{\sqrt{E_b} - b_i}{\sqrt{N_0}} \right) - erfc\left(\frac{\sqrt{E_b} - b_{i-1}}{\sqrt{N_0}} \right) \right]$$

$$P(r_k \in C_i | s_0) = P(y = y_i | x = 0) = \frac{1}{\sqrt{\pi N_0}} \int_{b_{i-1}}^{b_i} \exp\left\{ \frac{\left(r_k + \sqrt{E_b}\right)^2}{N_0} \right\} dr_k =$$

$$= \frac{1}{2} \left[erfc\left(\frac{\sqrt{E_b} + b_{i-1}}{\sqrt{N_0}} \right) - erfc\left(\frac{\sqrt{E_b} + b_i}{\sqrt{N_0}} \right) \right]$$

$i = 1.2, \ldots Q$ $\qquad b_0 = +\infty, \quad b_Q = -\infty$

where:

$$erfc(x) = \frac{2}{\sqrt{\pi}} \int_x^{\infty} e^{-t^2} \, dt$$

The unconditional probability that the received signal r_k falls into the interval C_i is therefore

$$P(y = y_i) = P(y = y_i | x = 1) P(x = 1) + P(y = y_i | x = 0) P(x = 0)$$

If we are unable to distinguish whether a 0 or a 1 was transmitted, we assume that the transmitted signals have equal probabilities:

$$P(x = 1) = P(x = 0) = 0.5$$

and therefore

$$P(y = y_i) = 0.5 \left[P(y = y_i | x = 1) + P(y = y_i | x = 0) \right]$$

For the symmetry, we have:

$$P(y = y_i) = P(y = y_{Q+1-i}) \qquad i = 1, \ldots, Q/2$$

and the probability of each quantization level is:

$$P_i = P(y = y_i) + P(y = y_{Q+1-i}) = 2P(y = y_i) =$$

$$\frac{1}{2}\left\{\left[Erfc\left(\frac{\sqrt{E_b} - b_i}{\sqrt{N_0}}\right) - Erfc\left(\frac{\sqrt{E_b} - b_{i-1}}{\sqrt{N_0}}\right)\right] + \left[Erfc\left(\frac{\sqrt{E_b} + b_{i-1}}{\sqrt{N_0}}\right) - Erfc\left(\frac{\sqrt{E_b} + b_i}{\sqrt{N_0}}\right)\right]\right\} \qquad \text{(A1)}$$

$i = 1, \ldots, Q\ 2.$

The soft decision thresholds are assumed to be equally spaced to meet the near optimum requirements of the Viterbi decoder [8]. Let us put

$$h_i = \frac{b_{Q/2-i}}{\sqrt{E_b}} \qquad i = 0, \ldots, Q/2$$

$$= \begin{cases} \dfrac{i}{Q/2} & i = 0, \ldots, Q/2 - 1 \\ +\infty & i = Q/2 \end{cases}$$

(A1) becomes:

$$P_i = \frac{1}{2}\left\{Erfc\left[\sqrt{\frac{E_b}{N_0}}(1 - h_i)\right] - Erfc\left[\sqrt{\frac{E_b}{N_0}}(1 - h_{i-1})\right] + Erfc\left[\sqrt{\frac{E_b}{N_0}}(1 + h_{i-1})\right] - Erfc\left[\sqrt{\frac{E_b}{N_0}}(1 + h_i)\right]\right\} =$$

$$\frac{1}{2}\left\{Erfc\left[10^{R/20}(1 - h_i)\right] - Erfc\left[10^{R/20}(1 - h_{i-1})\right] + Erfc\left[10^{R/20}(1 + h_{i-1})\right] - Erfc\left[10^{R/20}(1 + h_i)\right]\right\} = P_i(R)$$

$i = 1, \ldots, Q/2$

where R is the ratio E_b/N_0 expressed in dB.

APPENDIX B

In Fig. B1 a block diagram of the signal level estimator is shown. We suppose that after the demodulation, i.e. after the matched filter (MF), the signal is further filtered with a low-pass filter (LPF) whose noise equivalent bandwidth is B_l. The LPF output is then squared and converted to get the dB power level.

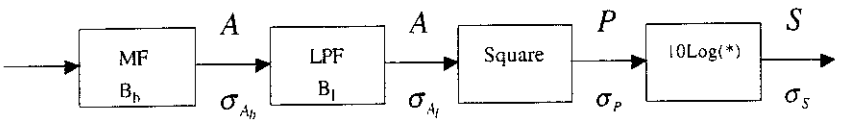

Fig. B1. Signal level estimator

Let us denote by A the signal rms amplitude present at the matched filter output and by B_b the signal noise equivalent bandwidth equal to $1/T_b$, where T_b is the bit duration. In the AWGN channel considered, A has a standard deviation $\sigma_{A_b} = \sqrt{\frac{N_0 B_b}{2}}$ which becomes

$$\sigma_{A_l} = \sqrt{\frac{N_0 B_l}{2}} \qquad \text{(B1)}$$

at the low pass filter output.

For small values of σ_{A_l} we can consider the filter output power $P = A^2$ as a Gaussian random variable with a standard deviation, σ_P, given by

$$\sigma_P = \sigma_{A_l} \frac{dP}{dA} = 2A\sigma_{A_l} \qquad \text{(B2)}$$

Substituting (B1) in (B2), the relative standard deviation , σ_P / P, is

$$\frac{\sigma_P}{P} = \frac{2\sigma_{A_l}}{A} = \frac{2\sqrt{\frac{N_0 B_l}{2}}}{\sqrt{E_b B_b}} = \sqrt{\frac{2N_0}{E_b \alpha}}$$

where α is the ratio B_b / B_l and $E_b = PT_b = P / B_b$ is the energy per bit of the signal.

For small values of the relative standard deviation σ_P / P we can consider the dB expression of the signal power $S = 10\,Log_{10} P$ as still being Gaussian with a standard deviation given by

$$\sigma_S = \sigma_P \frac{dS}{dP} = \frac{10}{Log_e 10} \frac{\sigma_P}{P} = 4.343 \sqrt{\frac{2N_0}{E_b \alpha}}$$

ACKNOWLEDGEMENTS

The authors wish to thank Dr. Mario Mauri from the CSTS (Centro Studi sulle Telecomunicazioni Spaziali) Institute for his collaboration.

REFERENCES

1. N. Celandroni, E. Ferro, N. James, F. Potortì
FODA/IBEA: a flexible fade countermeasure system in user oriented networks.
Intern. Journal of Satellite Communications, 10, No. 6, pp. 309-323, 1992.

2. N. Celandroni, E. Ferro, F. Potortì
The performance the FODA/IBEA satellite access scheme measured on the Italsat satellite.
Proc. of the ICDSC-10 Conference, pp. 332-338, V.1, Brighton 15-19 May 1995.

3. N. Celandroni, E. Ferro, F. Potortì, A. Bellini, F. Pirri
Practical experiences in interconnecting LANs via satellite.
To appear on the ACG SIGCOMM Computer Communication Review.

4. N. Celandroni, F. Potortì
Study of distributed algorithms for satellite channel capacity assignment in a mixed traffic and faded environment. Part II. The FEEDERS-TDMA proposal.
Submitted for publication in the International Journal on Satellite Communications, February 1995.

5. N. Celandroni, E. Ferro, F. Potortì
Comparison between distributed and centralised demand assignment TDMA satellite access schemes.
Submitted for publication in the International Journal on Satellite Communications, October 1995.

6. W. E. Leland, M. S. Taqqu, W. Willinger, D. V. Wilson
On the self-similar nature of Ethernet Traffic (extended version).
IEEE/ACM Transactions on Networking, Vol. 2, No. 1, February 1994.

7. Wing-Cheong Lau, A. Erramilli, J. L.Wang, W. Willinger
Self-Similar Traffic Generation: The Random Midpoint Displacement Algorithm and Its Properties.
ICC '95, Seattle, Washington USA, June 18-22 1995, pp. 466-472.

8. Y. Yasuda, Y. Hirata, A. Ogawa
Optimum Soft Decision for Viterbi Decoding.
IEEE 5th International Conference on Satellite Communications, Genova 1981.

9. H. Kazama, T.Atsugi, M. Umehira, S. Kato
A Feedback-Loop Type Transmission Power Control for Low Speed TDMA Satellite Communication Systems.
Proc.IEEE ICC '89, Boston MA.

10. E. Russo
Implementation of a space diversity system for Ka-band satellite communications.
IEEE ICC '93.

11. CCIR Report 564-4
Propagation data and prediction methods required for earth- space telecommunications systems. 1990.

12. L. Dossi, G. Tartara, E. Matricciani
Frequency diversity in millimeter wave satellite communications.
IEEE Trans. on Aerospace and Electronic Systems vol.28,n.2, pp.567-73, April 1992.

13. F. Carassa, E. Matricciani , G. Tartara
Frequency diversity and its applications.
International Journal of Satellite Communications, vol.6, pp.313-322 (1988).

14. F. Carassa
Technical aspects in the future development of satellite communication systems with particular reference to the use of frequencies above 10 GHz.
Proc. of the 19th Int.Conf. "Scientifico sullo spazio", Rome, March 1979, pp.22-41.

15. N. Celandroni
Estimation of the Eb/No ratio using PSK quantised levels in an additive white Gaussian noise (AWGN) environment.
CNUCE Report C90-22, September 1990.

16. D. Kreuer, E.Bierbaum
Improved Eb/No Estimation with Soft Quantized Detection.
Proc.PIMRC'94/WCN,Den Haag, The Netherlands, Sept. 1994, pp. 620-624.

17. J.S. Bendat, A.G. Piersol
Random Data: Analysis and Measurement Procedures.
Wiley and Sons, 1986.

18. R.V. Hogg, A.T. Craig
Introduction to Mathematical Statistics.
Prentice Hall, 1995.

19. A. Papoulis
Probability, Random Variables and Stochastic Processes.
McGraw-Hill, 1991

20. R.G. Brown, P.Y.C. Hwang
Introduction to Random Signals and Applied Kalman Filtering.
J. Wiley & Sons,1992.

21. B.D.O. Anderson
Optimal Filtering.
Prentice-Hall, 1979.

22. S.M. Bozic
Digital and Kalman Filtering.
Edward Arnold, 1979.

23. S. Benedetto, E. Biglieri, V. Castellani
Digital Transmission Theory.
Prentice-Hall, 1987.

24. J.G. Proakis
Digital Communications.
McGraw-Hill, 1995.

25. Peitgen, Jurgens, Saupe
Chaos and Fractals.
Springer-Verlag, New York 1992.

26. S. Wolfram
Mathematica: A System for Doing Mathematics by Computer.
Addison-Wesley, 1991.

27. R.L. Freeeman
Reference Manual for Telecommunications Engineering.
Wiley & Sons, 1995 Update.